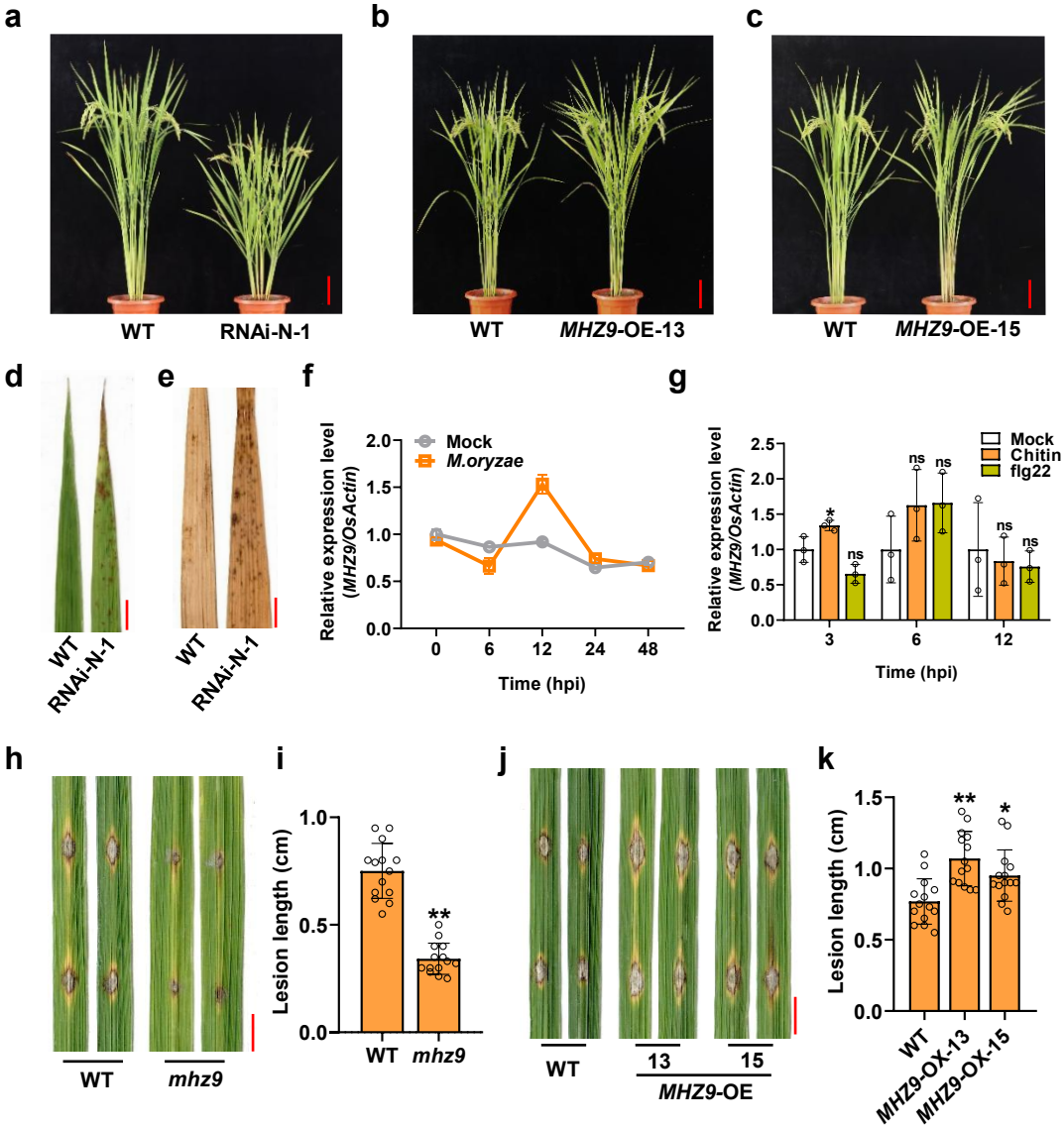

Supplementary Fig. 1 *MHZ9* acts as a negative regulator of immune responses in rice

a Field-grown phenotypes of *MHZ9* RNA interference (RNAi) plants (RNAi-N-1) at the heading stage. The sequence from the CDS of *MHZ9* (positions 668-1276 bp) was selected for plasmid construction of the RNAi vector. Bar = 10 cm.

b, c Field-grown phenotypes of WT and *MHZ9*-OE-13 and -15 transgenic lines at the heading stage. Scale bar = 10 cm.

d Detection of spontaneous lesions on leaves of WT and *MHZ9*-RNAi-N-1 plants at the heading stage. Bar = 1 cm.

e In situ detection of ROS in leaves of WT and *MHZ9*-RNAi-N-1 plants using DAB staining. Bar = 1 cm.

f Transcriptional analysis of *MHZ9* expression over time in rice after inoculation with *M. oryzae*. Conidial suspensions (5×10^5 conidia mL^{-1} in 0.02% Tween-20) were sprayed onto the leaf surfaces of two-week-old rice seedlings. Inoculated leaves were sampled at the indicated time points for RT-qPCR assays. 0.02% Tween-20 served as the mock treatment. Values are means ± SD (n = 3).

g Transcriptional analysis of *MHZ9* in rice suspension cells treated with 10 nM chitin or 500 nM flg22. RT-qPCR was performed to evaluate gene expression. Values are means ± SD (n = 3). * indicates significant differences mock at $P < 0.05$ (Student's *t*-test). ns, no significant difference.

h, i Disease symptoms of representative leaves (h) and lesion length (i) of WT and *mhz9* plants after punch inoculation with *M. oryzae*. Lesion lengths were measured, and photographs were captured at 5 dpi. Bar = 1 cm. Values are means ± SD (n = 3).

j, k Disease symptoms of representative leaves (j) and lesion length (k) from WT and *MHZ9*-OE-13/15 plants after punch inoculation with *M. oryzae*. Others are as in (h, i).

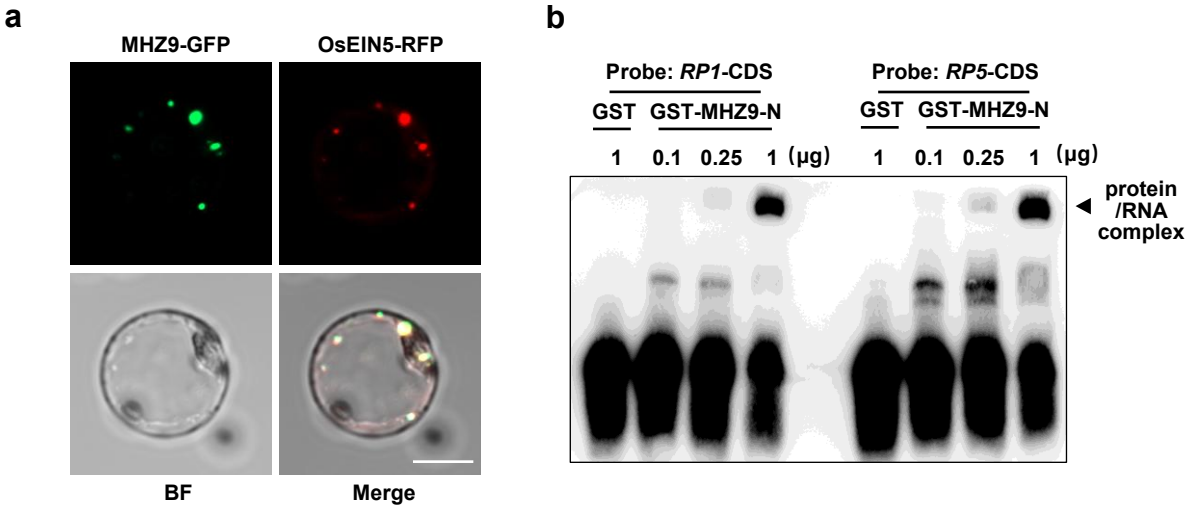

Supplementary Fig. 2 MHZ9 is localized to P-bodies and binds to defense-related mRNAs

a Colocalization of MHZ9-GFP and OsEIN5-RFP (P-body marker) in rice protoplasts. GFP, green fluorescent protein; RFP, red fluorescent protein; BF, bright field. Bar = 10 μm.

b The MHZ9-N exerted a dose-dependent binding activity to the *RP1* and *RP5* mRNAs. Protein/RNA complex bands were indicated by an arrow.

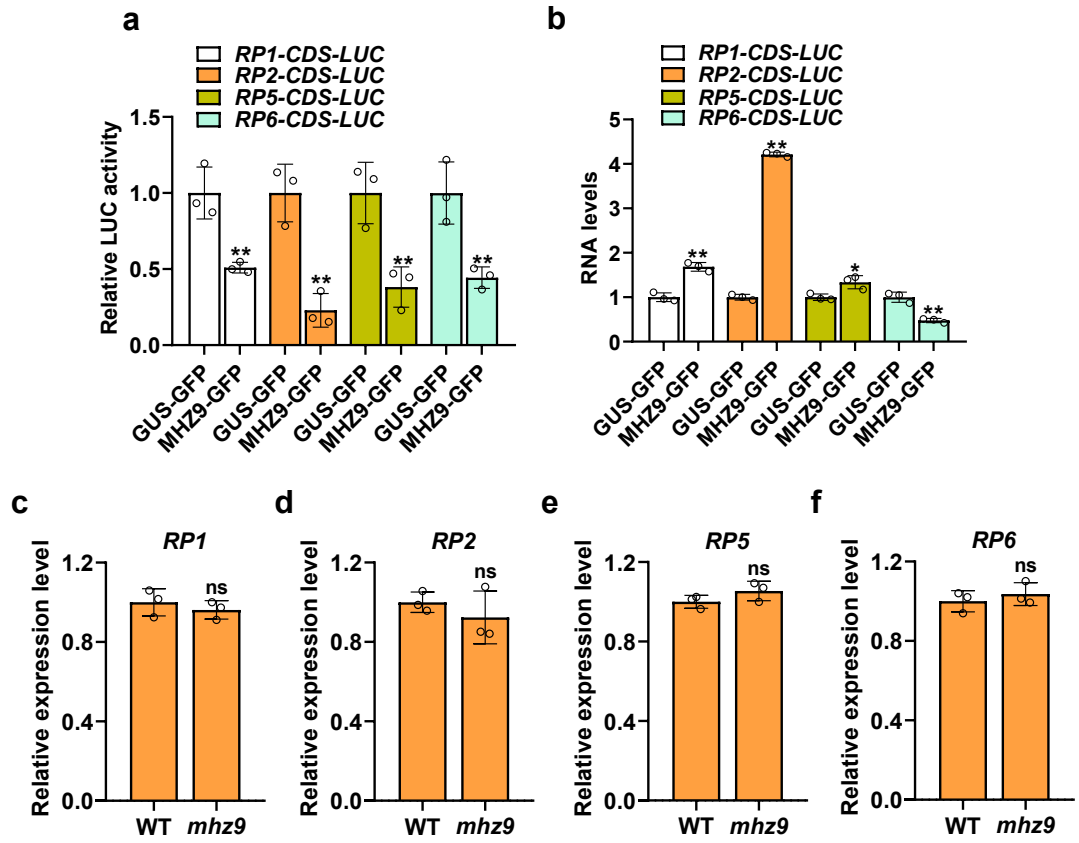

Supplementary Fig. 3 MHZ9 suppresses *RPs* translation

a, b MHZ9 effects on LUC activities and RNA levels of LUC fusions. Plasmids harboring both the reference *R-Luc* gene and the reporter *F-LUC* gene fused to the CDS of *RP1*/*2*/*5*/*6* were transiently transfected into *mhz9* protoplasts, together with either GUS-GFP or MHZ9-GFP. LUC activity was defined as the ratio of F-LUC to R-LUC. R-Luc served as a control (a). Relative RNA levels of LUC and its fused genes were analyzed by RT-qPCR, with R-Luc used for normalization (b). Values are means ± SD (*n* = 3).

c-f Relative transcript levels of *RP1* (c), *RP2* (d), *RP5* (e) and *RP6* (f) in WT or *mhz9* protoplasts. *OsActin* served as the internal reference gene. Values are means ± SD (*n* = 3).

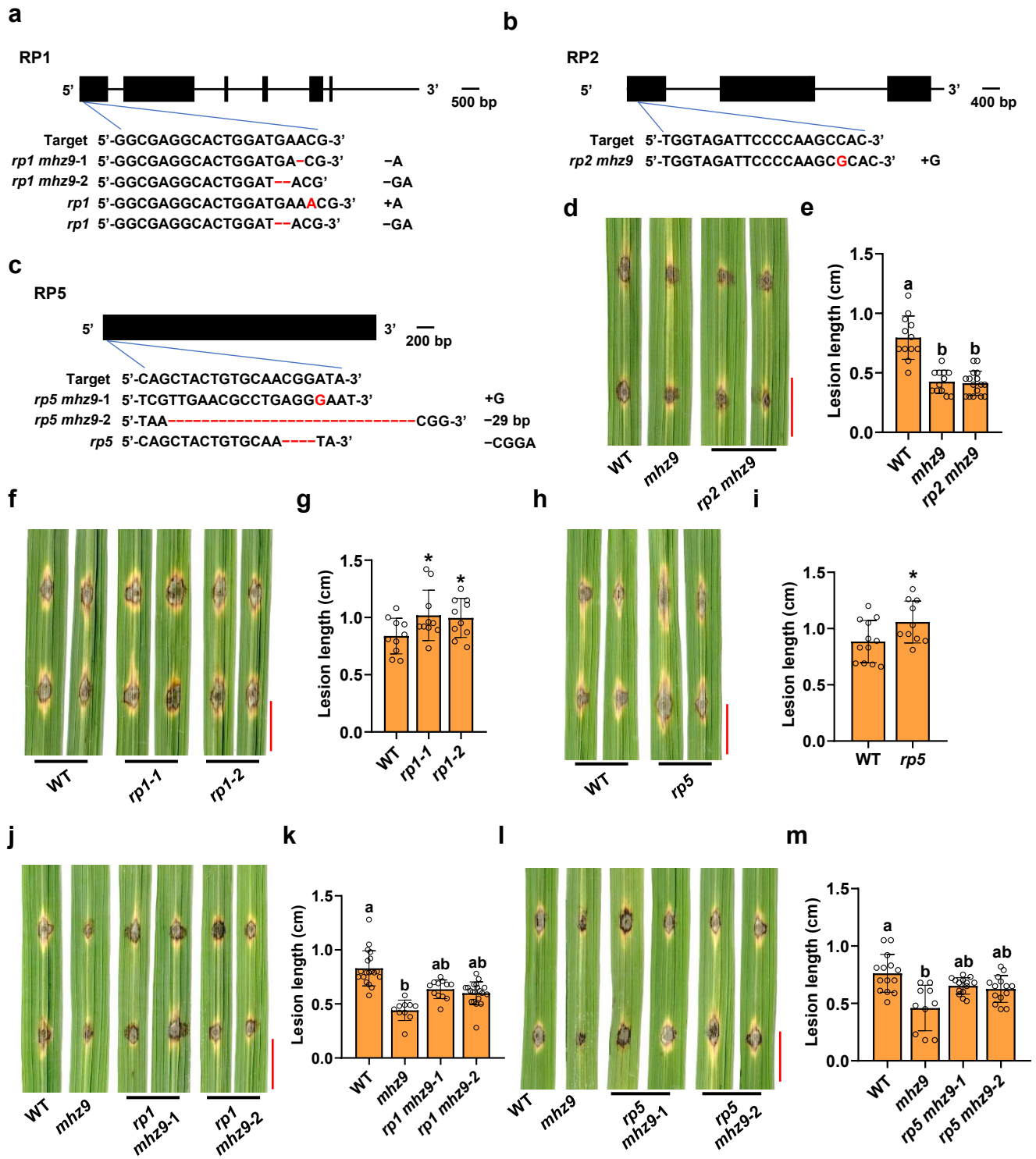

Supplementary Fig. 4 Loss of *RP1* or *RP5* function can partially abrogate the enhanced disease resistance phenotype of *mhz9*

a-c Diagram of the mutation types in *rp1* (a), *rp2* (b), and *rp5* (c) mutant lines generated by CRISPR/Cas9.

d, e Disease symptoms of representative leaves (d) and lesion length (e) of WT and *rp2 mhz9* double mutant plants after punch inoculation with *M.oryzae* strain 18-zx-51 (8×10^5 conidia mL^{-1} in 0.02% Tween 20). Lesion lengths were measured, and photographs were captured at 5 days dpi. Bar = 1 cm. Values are means ± SD (n = 3).

f, g Disease symptoms of representative leaves (f) and lesion length (g) of WT and *rp1*-1/2 plants after punch inoculation with *M. oryzae*. Others are as in (d, e).

h, i Disease symptoms of representative leaves (h) and lesion length (i) of WT and *rp5* plants after punch inoculation with *M. oryzae*. Others are as in (d, e).

j, k Disease symptoms of representative leaves (j) and lesion length (k) from WT and *rp1 mhz9*-1/2 plants after punch inoculation with *M. oryzae*. Others are as in (d, e).

l, m Disease symptoms of representative leaves (l) and relative leaf area with lesions (m) from WT and *rp5 mhz9*-1/2 plants after punch inoculation with *M. oryzae*. Others are as in (d, e).

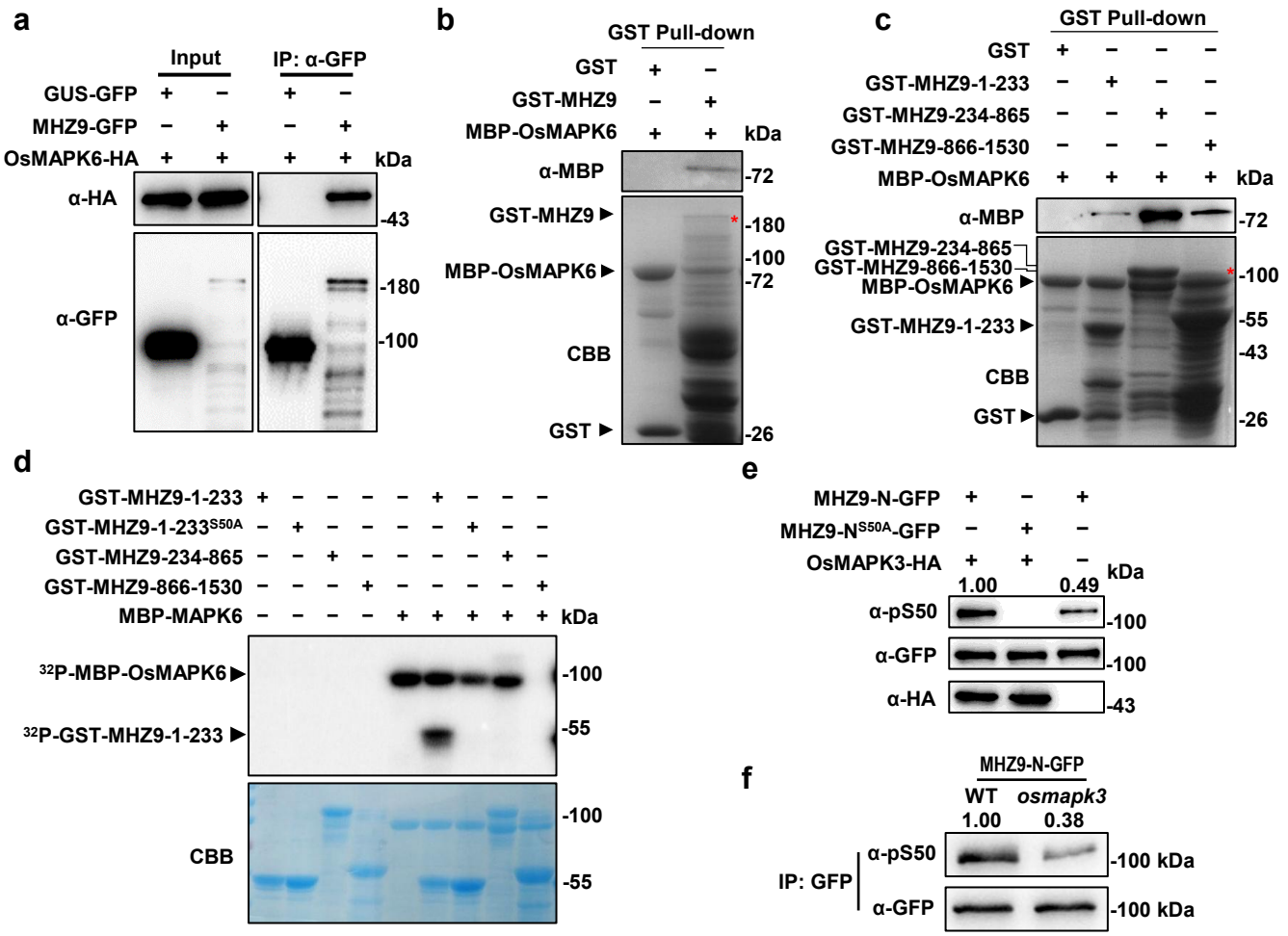

Supplementary Fig. 5 MHZ9 interacts with OsMAPK6 and is phosphorylated at Ser50

a Co-IP assays confirming the interaction between MHZ9 and OsMAPK6. MHZ9-GFP, GUS-GFP, and OsMAPK6-HA were co-expressed in rice protoplasts. Extracted proteins were immunoprecipitated with anti-GFP beads, and Co-IP proteins were immunoblotted with an anti-HA antibody.

b GST pull-down assays demonstrating the interaction between MHZ9 and OsMAPK6. Recombinant GST-MHZ9 and MBP-OsMAPK6 were purified from *E. coli* and subjected to GST pull-down assays. CBB staining indicates protein abundance; GST served as a negative control.

c GST pull-down assays showing the interaction between OsMAPK6 and various MHZ9 truncations. Others are as in (b).

d In vitro phosphorylation assays to determine whether OsMAPK6 phosphorylates various MHZ9 truncations and sites. Protein phosphorylation was detected by autoradiography (upper panel); protein loading is indicated by CBB staining (lower panel).

e In vivo phosphorylation of MHZ9-N at Ser50 by OsMAPK3, detected by immunoblotting with an antibody specifically recognizing phosphorylated Ser50 of MHZ9-N. Numbers indicate relative protein levels normalized to GFP. Relative band intensities from immunoblots were quantified using ImageJ.

f In vivo phosphorylation of MHZ9-N at Ser50 in WT and *osmapk3*. MHZ9-N-GFP was transiently transfected into WT and *osmapk3* protoplasts. Phosphorylation of MHZ9-N at Ser50 was examined by immunoblotting using the anti-pS50 antibody. Relative band intensities from immunoblots were quantified using ImageJ.

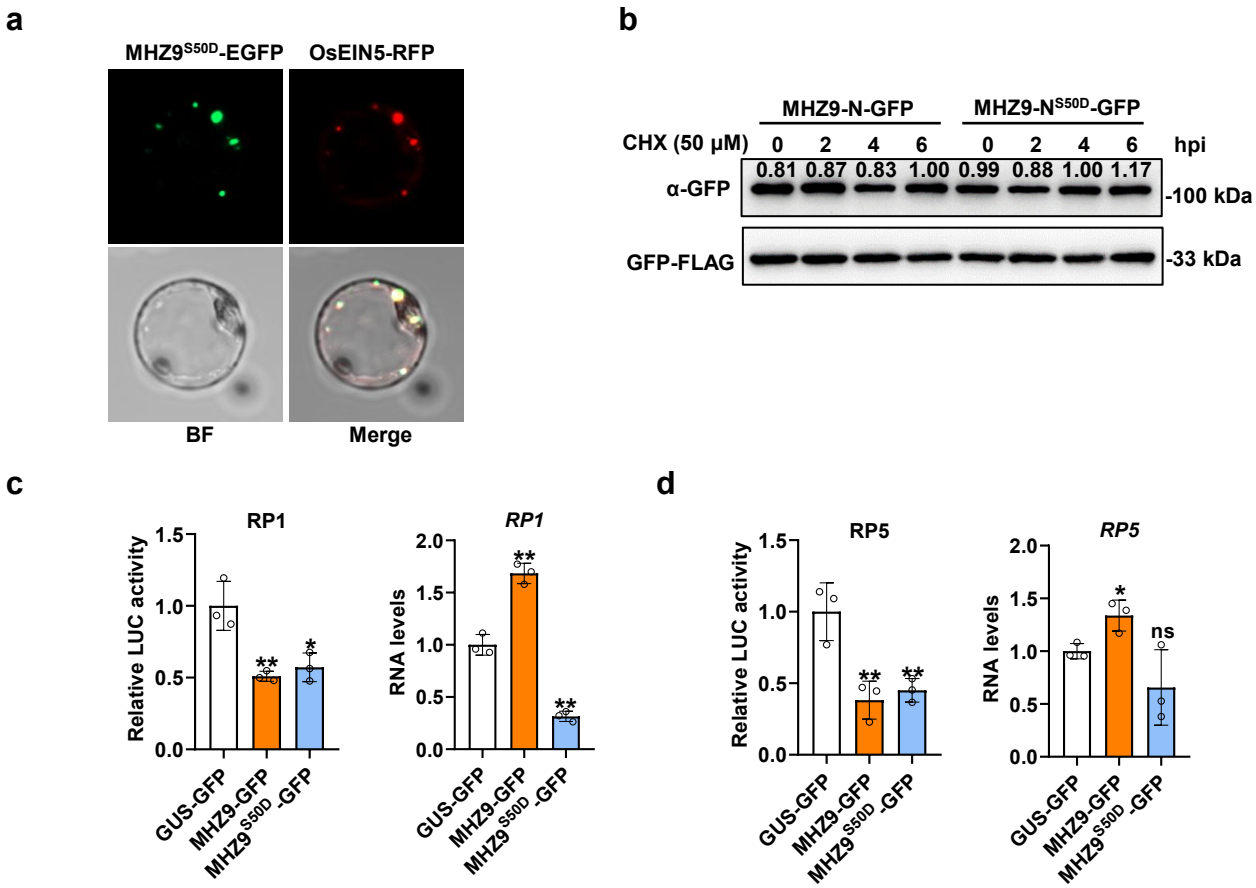

Supplementary Fig.6 Ser50 phosphorylation does not alter MHZ9 subcellular localization or protein stability

a Colocalization assays of MHZ9^{S50D} and OsEIN5 (P-body marker) in rice protoplasts. Bar = 10 μm.

b Protein stability analysis of MHZ9-N upon Ser50 phosphorylation. MHZ9-N-GFP or MHZ9-N^{S50D}-GFP was transiently expressed in rice protoplasts for 14 h, followed by treatment with the protein synthesis inhibitor cycloheximide (CHX, 50 μM) for the indicated times. Protoplasts were then collected for protein extraction, and protein abundance was detected by immunoblotting with the indicated antibodies. GFP-FLAG was transiently co-expressed as an internal control. Relative band intensities from immunoblots were quantified using ImageJ.

c, d MHZ9 and MHZ9^{S50} effect on LUC activities and RNA levels of LUC fusions. The plasmid harboring both the reference *R-Luc* gene and the reporter *F-LUC* gene fused to the CDS of *RP1* (c) or *RR5* (d) was transiently expressed in protoplasts. LUC activity was defined as F-LUC/R-LUC. F-LUC was used as a control (left). Relative RNA levels of LUC and its fused genes were analyzed through RT-qPCR. R-LUC was used for normalization (right). Values are means ± SD (n = 3). Asterisks indicate significant differences using the two-tailed Student's t-test (*P < 0.05 and **P < 0.01). Ns, no significant.

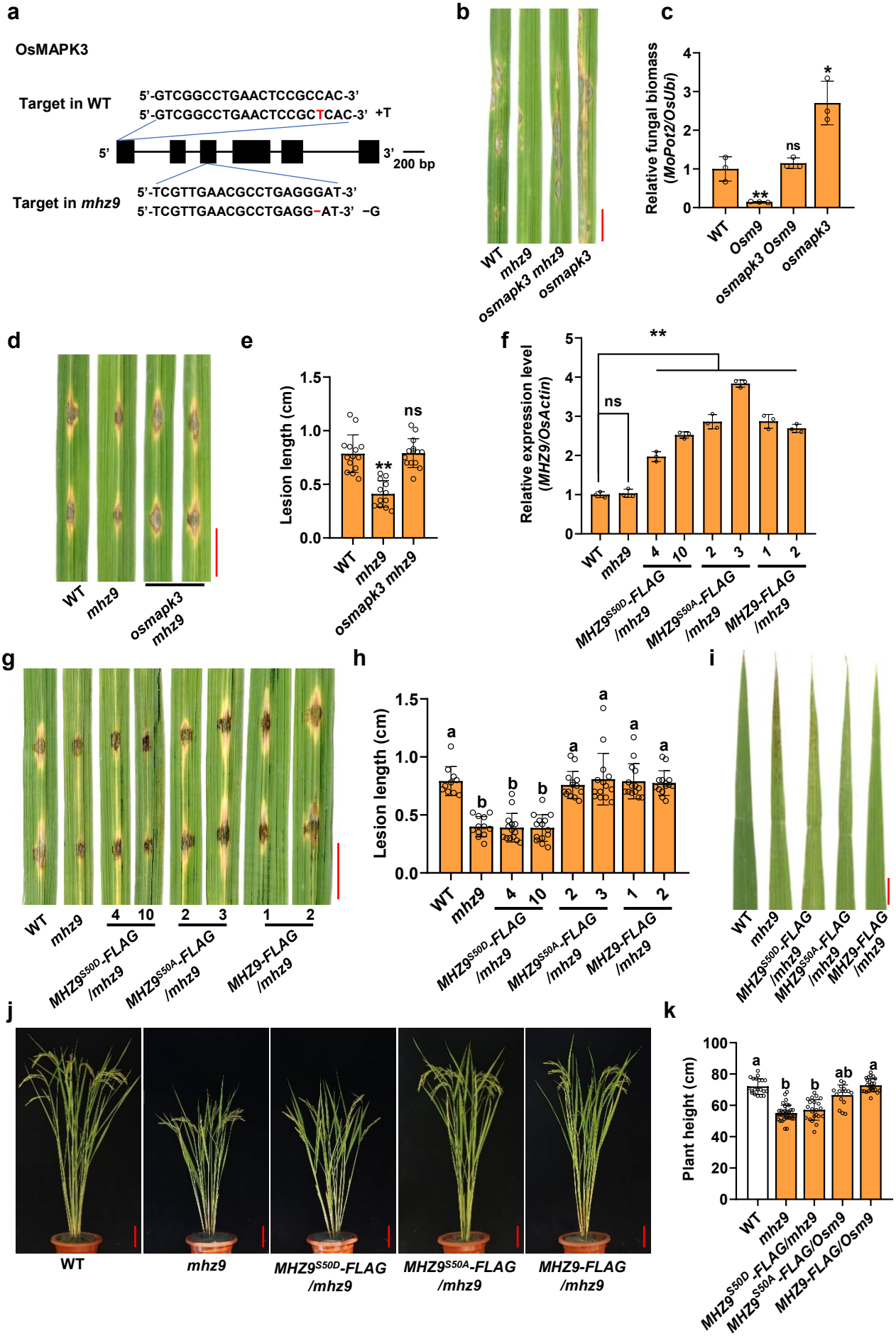
a
OsMAPK3
Target in WT
5'-GTCGGCCTGAACTCCGCCAC-3'
5'-GTCGGCCTGAACTCCGCTCAC-3' +T
5'
3'
200 bp
Target in mhz9
5'-TCGTTGAACGCCTGAGGGAT-3'
5'-TCGTTGAACGCCTGAGG−AT-3' −G
b
WT
mhz9
osmapk3 mhz9
osmapk3
c
Relative fungal biomass (MoPot2/OsUbi)
ns
WT
Osm9
osmapk3 Osm9
osmapk3
d
WT
mhz9
osmapk3 mhz9
e
Lesion length (cm)
ns
WT
mhz9
osmapk3 mhz9
f
Relative expression level (MHZ9/OsActin)
ns
WT
mhz9
MHZ9S50D-FLAG /mhz9
MHZ9S50A-FLAG /mhz9
MHZ9-FLAG /mhz9
g
WT
mhz9
MHZ9S50D-FLAG /mhz9
MHZ9S50A-FLAG /mhz9
MHZ9-FLAG /mhz9
h
Lesion length (cm)
i
WT
mhz9
MHZ9S50D-FLAG /mhz9
MHZ9S50A-FLAG /mhz9
MHZ9-FLAG /mhz9
j
WT
mhz9
MHZ9S50D-FLAG /mhz9
MHZ9S50A-FLAG /mhz9
MHZ9-FLAG /mhz9
k
Plant height (cm)
WT
mhz9
MHZ9S50D-FLAG/mhz9
MHZ9S50A-FLAG/Osm9
MHZ9-FLAG/Osm9

Supplementary Fig. 7 Ser50 phosphorylation-mediated inactivation of MHZ9 confers blast resistance but compromises growth in rice

a Diagram of mutation types in *osmapk3* mutant lines generated by CRISPR/Cas9.

b, c Disease symptoms of representative leaves (b) and relative fungal biomass (c) of two-week-old WT, *mhz9, osmapk3* and *osmapk3 mhz9* plants after spray inoculation with *M. oryzae*. Images were taken at 5 dpi. Relative fungal biomass was determined by qPCR. Bar = 1 cm. Values are means ± SD (*n* = 3).

d, e Disease symptoms of representative leaves (d) and lesion length (e) of four-week-old WT, *mhz9* and *osmapk3 mhz9* plants after punch inoculation with *M. oryzae*. Lesion lengths were measured, and photographs were taken at 5 dpi. Bar = 1 cm. Values are means ± SD (*n* = 3).

f Relative transcript levels of *MHZ9* in WT, *mhz9*, and transgenic lines overexpressing *MHZ9-FLAG* (1 and 2), *MHZ9^{S50D}-FLAG* (4 and 10), and *MHZ9^{S50A}-FLAG* (2 and 3) in the *mhz9* mutant were detected using RT-qPCR. *OsActin* was used as the internal control. Values are means ± SD (*n* = 3).

g, h Disease symptoms of representative leaves (g) and lesion length (h) of four-week-old WT, *mhz9* and transgenic lines overexpressing *MHZ9-FLAG* (1 and 2), *MHZ9^{S50D}-FLAG* (4 and 10), and *MHZ9^{S50A}-FLAG* (2 and 3) in the *mhz9* mutant plants after punch inoculation with *M. oryzae*. Lesion lengths were measured, and photographs were taken at 5 dpi. Bar = 1 cm. Different letters indicate the significant differences based on a two-factor ANOVA with Tukey's HSD test ($P < 0.05$, Data are means ± SD, *n = 3* biological replicates).

i Detection of Spontaneous lesions in WT, *mhz9* and transgenic lines overexpressing *MHZ9-FLAG* (1 and 2), *MHZ9^{S50D}-FLAG* (4 and 10), and *MHZ9^{S50A}-FLAG* (2 and 3) in the *mhz9* mutant leaves at the heading stage. Bar = 1 cm.

j, k Phenotypes of WT and different transgenic plants at the heading stage (j) and plant height at mature stage (k). Bar = 10 cm**.** Different letters indicate the significant differences based on a two-factor ANOVA with Tukey's HSD test ($P < 0.05$, Data are means ± SD, *n = 3* biological replicates).